Environmental Pollution 294 (2022) 118662

Contents lists available at ScienceDirect

Environmental Pollution

journal homepage: www.elsevier.com/locate/envpol

# Polystyrene microbeads influence lipid storage distribution in *C. elegans* as revealed by coherent anti-Stokes Raman scattering (CARS) microscopy☆

Hendrik Fueser [a,*], Christian Pilger [b], Cihang Kong [b], Thomas Huser [b], Walter Traunspurger [a]

[a] Bielefeld University, Animal Ecology, Konsequenz 45, 33615, Bielefeld, Germany
[b] Bielefeld University, Biomolecular Photonics, Universitätsstraße 25, 33615, Bielefeld, Germany

ARTICLE INFO

*Keywords:*
Polystyrene beads
Microspheres
Microplastics
Nematodes
Food dilution
Coherent anti-Stokes Raman scattering (CARS)

ABSTRACT

The exposure of *Caenorhabditis elegans* to polystyrene (PS) beads of a wide range of sizes impedes feeding, by reducing food consumption, and has been linked to inhibitory effects on the reproductive capacity of this nematode, as determined in standardized toxicity tests. Lipid storage provides energy for longevity, growth, and reproduction and may influence the organismal response to stress, including the food deprivation resulting from microplastics exposure. However, the effects of microplastics on energy storage have not been investigated in detail. In this study, *C. elegans* was exposed to ingestible sizes of PS beads in a standardized toxicity test (96 h) and in a multigeneration test (~21 days), after which lipid storage was quantitatively analyzed in individual adults using coherent anti-Stokes Raman scattering (CARS) microscopy. The results showed that lipid storage distribution in *C. elegans* was altered when worms were exposed to microplastics in form of PS beads. For example, when exposed to 0.1-μm PS beads, the lipid droplet count was 93% higher, the droplets were up to 56% larger, and the area of the nematode body covered by lipids was up to 79% higher than in unexposed nematodes. The measured values tended to increase as PS bead sizes decreased. Cultivating the nematodes for 96 h under restricted food conditions in the absence of beads reproduced the altered lipid storage and suggested that it was triggered by food deprivation, including that induced by the dilutional effects of PS bead exposure. Our study demonstrates the utility of CARS microscopy to comprehensively image the smaller microplastics (<10 μm) ingested by nematodes and possibly other biota in investigations of the effects at the level of the individual organism.

## 1. Introduction

In freshwaters, microplastics (MPs) have been found in a near infinite number of shapes and colors (e.g., Rios Mendoza and Balcer, 2019) and data on the environmental concentrations is either incomplete or varies widely between environmental compartments and MP sizes. In aquatic systems, as a result of fragmentation and sedimentation processes, the concentrations of plastic fragments are often higher in sediments than in the water phase, such that sediments are considered as sinks for MPs (Scherer et al., 2020; Wendt-Potthoff et al., 2014).

Among benthic meiofauna organisms, nematodes are the dominant taxon, with high abundances in freshwater, marine, and terrestrial environments worldwide (Heip et al., 1990; Traunspurger, 2021; van den Hoogen et al., 2019). And with their lifestyle in aerobic sediment layers, nematodes are directly and continuously exposed to sediment pollutants (Traunspurger et al., 2012; Traunspurger et al., 2020) over their entire life span (Höss et al., 2011). Among the limited studies focusing on MP ingestion by nematodes (Fueser et al., 2020a), the most thoroughly investigated species has been the model organism *Caenorhabditis elegans* (Fang-Yen et al., 2009; Fueser et al., 2020b; Kiyama et al., 2012; Lei et al., 2018; Zhao et al., 2017) showing that *C. elegans* is able to readily ingest MPs ≤3.4 μm (Boyd et al., 2003; Fueser et al., 2019).

In the study by Mueller et al. (2020b), using micron-sized polystyrene (PS) beads (diameters: 0.1, 0.5, 1.0, 3.0, 6.0 and 10.0 μm), negative effects on the reproduction of *C. elegans* were observed that increased with increasing exposure concentrations and decreasing bead diameters as demonstrated in standardized single-species 96-h chronic toxicity tests (following ISO10872). In addition, multigeneration tests revealed that lower concentrations of 1.0-μm PS beads but a continuous exposure for up to 49 days induced subtle changes in nematode

☆ This paper has been recommended for acceptance by Eddy Y. Zeng.

* Corresponding author.
*E-mail address:* h.fueser@uni-bielefeld.de (H. Fueser).

https://doi.org/10.1016/j.envpol.2021.118662
Received 29 August 2021; Received in revised form 4 December 2021; Accepted 7 December 2021
Available online 8 December 2021

population dynamics (population growth rates; Mueller et al., 2020a). Moreover, PS beads of 6.0 and 10.0 μm in diameter, while too large to be ingested by *C. elegans*, also significantly affected reproduction. Similar indirect effects have thus far mainly been described for other taxa, such as crustaceans and annelids (Aljaibachi et al., 2020; Besseling et al., 2013; Blarer and Burkhardt-Holm, 2016; Ogonowski et al., 2016). In *C. elegans*, the mechanism may involve a dilution of the nematode's bacterial diet by the MPs, thereby reducing food availability and feeding efficiency (Rauchschwalbe et al., 2021) and thus disturbing intestinal function (Shang et al., 2020). With less food consumed by nematodes exposed to PS beads, the resulting undernourishment should be evidenced by differences in lipid storages compared to unexposed nematodes.

Vibrational spectroscopic techniques such as Raman microscopy are well-suited for lipid storage analyses. In spontaneous Raman scattering spectroscopy, the radiation from a monochromatic light source (laser) interacts with the aliphatic sample (e.g., polymers and the fatty acid chains of lipids) by the inelastic scattering of a small proportion of photons. The resulting shift in their energy provides information about the vibrations of a molecule in the form of a vibrational spectrum (e.g., Araujo et al., 2018; Käppler et al., 2016). However, a more efficient approach is coherent anti-Stokes Raman scattering (CARS) microscopy, which overcomes the low signal intensity of Raman spectroscopy by employing multiple photons to actively drive the molecular bond vibration of interest, thus producing a coherent, resonance-enhanced signal in a pump-probe experiment (e.g., Ribeiro-Claro et al., 2016). The use of non-invasive, label-free CARS microscopy has allowed imaging of the distribution of lipid droplets in the tissues of *C. elegans*, based on signal probing of the aliphatic 2845 $cm^{-1}$ $CH_2$ stretching vibration of fatty acid chains (Evans and Xie, 2008) that functions as a general marker of lipids (e.g., Chen et al., 2020; Fueser et al., 2018; Hellerer et al., 2007; Smus et al., 2017; Wang et al., 2014; Yen et al., 2010; Yi et al., 2014). CARS microscopy has also been employed to detect alterations in lipid storage distribution induced by exposure of the organism to contaminants (e.g., Fueser et al., 2018) or to MPs (e.g., Rummel et al., 2017; Welden and Cowie, 2016; Yang et al., 2020) and to detect smaller MPs in zooplankton (Cole et al., 2013), crabs (Watts et al., 2014), fairy shrimp and zebrafish embryos (Galloway et al., 2017).

Because their body is transparent to light, nematodes transmit strong Raman signals, such that lipid storage and ingested MPs <10 μm can be imaged simultaneously. Thus, in this study, we used CARS microscopy to quantitatively investigate the distribution of lipid droplets in fixed (formaldehyde 4%) samples of adult *C. elegans* that had been exposed or not (controls) to high effective PS bead concentrations (EC50) in 96-h chronic toxicity tests following Mueller et al. (2020b) and to lower PS bead concentrations in multigeneration tests (see Mueller et al., 2020a). We hypothesized that stress-induced lipid storage distribution in *C. elegans* is the same whether the stress is food deprivation or the ingestion of PS beads together with bacterial cells. To test this hypothesis, lipid storage in nematodes cultured under conditions of an ideal ($10^9$ *E. coli* cells $ml^{-1}$) or a restricted ($10^7$ *E. coli* cells $ml^{-1}$) food density was additionally examined using CARS microscopy.

## 2. Material and methods

### 2.1. Test organism

*C. elegans* was provided as a starting culture by the Caenorhabditis Genetics Center (University of Minnesota, Minneapolis, MN, USA). The nematodes were further cultivated on agar plates containing nematode growth medium and *Escherichia coli* OP50 following the standard procedures described in Stiernagle (2006). The culture plates were stored at 20 °C in the dark until needed.

### 2.2. Experimental procedures

In the lipid analyses of *C. elegans* by CARS microscopy, the nematodes were subjected to chronic toxicity tests following ISO10872 (Mueller et al., 2020b) and to multigeneration tests (Mueller et al., 2020a).

Briefly, in the single-species chronic toxicity test J1 juveniles of *C. elegans* in standard cell culture plates (cell growth area per well: 3.85 $cm^2$; VWR International GmbH, Darmstadt, Germany) were exposed to 0.1-μm, 0.5-μm, and 1.0-μm PS beads prepared in aqueous medium to obtain exposure concentrations of 54.9 mg $l^{-1}$, 687 mg $l^{-1}$, and 549 mg $l^{-1}$, respectively, that correspond with the effective concentration inhibiting the reproduction of *C. elegans* by 50% (EC50) since analyses of the cultures after 96 h of incubation showed dose-dependent and PS bead size-dependent inhibitory effects on reproduction (Mueller et al., 2020a). Seven adult *C. elegans* per PS bead size treatment (28 nematodes in total) were randomly chosen and preserved in 4% formaldehyde until they were imaged with CARS microscopy.

The multigeneration test of *C. elegans* was conducted in semi-fluid medium spiked with 5.49 mg 1.0-μm PS beads $l^{-1}$, which corresponded to 1% of the concentration that induced 50% inhibition on *C. elegans'* reproduction after 96 h exposure (Mueller et al., 2020b). Analyses of the cultures after 21 days revealed the subtle impacts of continuous PS bead exposure on nematode population dynamics (Mueller et al., 2020b), including a significant decrease in the carrying capacity but also effects on population growth rates, population doubling time, and the time needed to reach the maximum sustainable yield. Ten adult *C. elegans* randomly chosen from the PS bead and from the control treatments were preserved in 4% formaldehyde until they were imaged with CARS microscopy.

PS beads were chosen as representative microplastic particles because they are a common plastic polymer type and form of microplastics <200 μm, with high environmental quantities determined at microplastic "hot spot" sampling sites, including in riverine sediments (e.g., Scherer et al., 2020). PS beads with diameters close to the size of *E. coli* cells were previously shown to be readily ingested by *C. elegans* (e.g, Fueser et al., 2019; Mueller et al., 2020b). All applied PS bead stock suspensions were checked regarding the bead's polymer type, form, size distribution, density and surface charge and corresponded well with the manufacturer specifications (characterized in Mueller et al., 2020b). Additionally, to determine lipid distributions under ideal and restricted food conditions, J1 juveniles were placed in the wells of a standard cell culture plate (cell growth area per well: 3.85 $cm^2$; VWR International GmbH) and cultured for 96 h in the presence of *E. coli* suspended in K-medium (3.1 g NaCl $l^{-1}$, 2.4 g KCl $l^{-1}$) to achieve densities of either $10^9$ cells $ml^{-1}$ (ideal food density) or $10^7$ cells $ml^{-1}$ (restricted food density). Ten adult *C. elegans* were randomly chosen from each of the two food density treatments and preserved in 4% formaldehyde until they were imaged with CARS microscopy.

### 2.3. Imaging lipid storage distributions by CARS microscopy

Label-free CARS microscopy was performed using a lab-built laser scanning microscope. The feature of the microscope are as follows: A 2-ps pulsed fiber-based laser (Emerald Engine, APE) with a central wavelength of 1032 nm and an 80-MHz repetition rate provides the fundamental Stokes beam at a fixed wavelength and is frequency doubled to 516 nm. The frequency-doubled laser light pumps an optical parametric oscillator (OPO; Levante Emerald, APE) that generates tunable laser wavelengths that serve as the pump beam in the CARS experiment. Based on the selected wavelengths combination of the Stokes beam (1032 nm) and the tuneable pump laser beam (~798 nm), the desired molecular bond vibration can be targeted for imaging. The temporal and spatial overlap of the laser beams is achieved using dichroic mirrors and an optical delay stage. To avoid detrimental effects to the nematode samples, a total focal power of <35 mW is used for all

images. This focal power proved to be suitable for long term investigations of *C. elegans* without causing notable harm to the nematodes as demonstrated by the continuous imaging over more than 60 min during which the nematodes moved and behaved without any visible impairment. The beams are raster scanned over the sample in a line-by-line manner using a galvanometric scanning mirror pair (model 6215H, Cambridge Technology) and focused into the sample by a 60 × water immersion objective lens (UPlanSApo, NA = 1.2, Olympus). The photons are collected by a condenser lens (U-AAC, NA = 1.4, Olympus, Germany) in a 4-pi configuration. Lipids are determined by targeting the 2845 $cm^{-1}$ $CH_2$ vibration (in aliphatic chains), considered to be a general biomarker of fatty acids. PS is imaged by exciting the 3050 $cm^{-1}$ bond vibration (aromatic C–H group). To filter out undesired wavelengths such as the pump and Stokes beams or auto-fluorescence signals, a stack comprising optical short-pass (SP) and bandpass (BP) filters is inserted in the beam path behind the condenser lens to isolate CARS signals occurring at 650 nm (lipids) and 633 nm (PS/plastic). The CARS signal is detected with the aid of a photomultiplier tube (PMT) (H 9656–20, Hamamatsu Photonics) and transferred into an electric signal, which is then finally recorded by an analog-to-digital converter (PCI–6110 S, National Instruments). The imaging process is controlled using the MATLAB-based program ScanImage 3.8 (Pologruto et al., 2003), which is also performing the correlation of the scanning mirror position and the PMT signal and transfers this into the final image. The z-stacks are performed by an automated routine that controls a closed-loop piezo-driven sample stage (S/N 222,009, Märzhäuser). In this study, nematodes were removed from the preserved samples and individually placed in the wells of a custom-built stainless-steel 27-well microscopic slide (7.0 × 3.5 cm; well diameter: 4-mm, glass bottom thickness: 170-μm), with each well containing 10 μl of phosphate-buffered saline. The nematodes were then individually imaged for lipid quantitation by CARS microscopy at a highly recognizable position: the vulva region. Depending on the nematode's body diameter, z-stacks (step size: 1 μm) consisting of 16–64 slices exhibiting lipid droplets were collected. The field of view in each of the images covered an area of 150 × 150 μm. The scanning speed of each image was 8 ms per line (pixel dwell time of 12.8 μs), while 512 × 512 pixels were acquired (total acquisition time per image: 3.35 s). In the current configuration this setup offers a lateral resolution of 350 nm and an axial resolution of 500 nm.

### 2.4. Method of analyzing lipid quantities in ImageJ

Lipid droplet distribution and content were analyzed in the z-stacks of 63 specimens with the open-source software *ImageJ* (Schneider et al., 2012) to determine the lipid droplet count, the total lipid area, the average lipid droplet size, and the percent area of the worm occupied by lipid stores. Briefly, single CARS microscopy images were transferred to image stacks and by using the projection function (projection type: max intensity) all CARS signal intensity was summed up into a two-dimensional image. All two-dimensional lipid signals dropped off within the width of the laser foci (approx. 400 nm), indicating a distinct border between the lipid droplet and the cytoplasm. Now with the adaptive thresholding function (Hellerer et al., 2007; Yi et al., 2014) the images were segmented into features of interest (here lipid droplets, using a white value range of 250–650) and background. The thresholded features are then displayed in red and with the particle analyzer tool of ImageJ the features were measured individually. Therefore, a correction factor with a threshold of 1 $\mu m^2$ was defined to exclude all potential artifacts not caused by lipid signals. Finally, the total lipid area was calculated by summing up the individual areas of lipid droplets and the percent area of the worm occupied by lipid stores by dividing the total area of lipids by the total area of the nematode shown in the image section. For illustration purposes z-projections were provided with the Gaussian blur filter and the lookup table "Fire".

### 2.5. Statistical analysis

The data were checked for normality (Shapiro-Wilk test) and homogeneity of variance (Levene test) but were not transformed. Data used in the lipid analysis were subjected to a one-way analysis of variance (ANOVA) on ranks (post-hoc: Dunn's method) or Mann-Whitney rank sum tests as indicated in the figures to compare the total area occupied by lipids, the lipid area fraction, and the average size of the lipid droplets in PS-bead-exposed vs. unexposed nematodes. A p-value $< 0.05$ was defined as significant in all comparisons. All statistical analyses were performed using SigmaPlot 12.0 (Systat Software Inc.).

## 3. Results

In CARS microscopy, MPs can be easily visualized and quantified by signal probing of the specific CH stretching vibration. PS is detected at 3050 $cm^{-1}$ which is associated with the aromatic ring. The transparent body of *C. elegans* enables the selective detection of both fluorescently labelled and unlabelled PS beads in the nematode's intestine. At relatively high exposure concentrations, PS beads were readily ingested by *C. elegans,* and high MP burdens were seen throughout its intestine, with accumulation of the beads where intestinal flow was slower, such as behind the terminal bulb and in the post-intestine before the rectum (Fig. 1). In nematodes exposed to high PS bead concentrations in the chronic toxicity tests, body deformations at the rectum were apparent (Fig. 1; for comparison with a normal rectum form see Fig. S1).

### 3.1. Caenorhabditis elegans exposed to 0.1-, 0.5-, and 1.0-μm PS beads in a 96-h chronic toxicity test

In nematodes from the chronic toxicity test, exposure for 96 h (during which time the worms grew from J1 to adults) to 0.1-, 0.5-, or 1.0-μm PS beads revealed an influence on lipid droplet distribution between PS bead-exposed and control nematodes. While there was only a significant difference in the number of lipid droplets between the control and PS bead-exposed nematodes on the basis of a significance level of

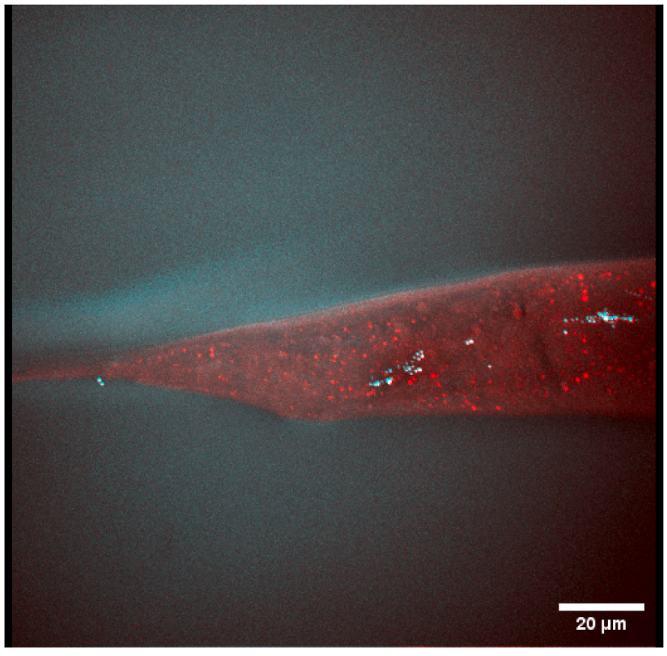


**Fig. 1.** Detection of lipid droplets (red; 2845 $cm^{-1}$) and ingested polystyrene beads (cyan; 3050 $cm^{-1}$; here 1.0 μm) in adult *Caenorhabditis elegans*. Z-projection of a z-stack covering a depth of 63 μm (step size: 1 μm). Field of view: 150 × 150 μm. Scale bar: 20 μm. (For interpretation of the references to color in this figure legend, the reader is referred to the Web version of this article.)

10% (Fig. 2A), lipid droplets were significantly larger (+47%; H = 10.519; p = 0.015; Fig. 2B and C) and the proportion of the nematode covered by those droplets (Fig. 2D) was significantly larger (+79%; H = 11.593; p = 0.008) in nematodes exposed to 0.1-μm PS beads (significance level: 5%). Moreover, the total lipid area, the average lipid droplet size and the percentage lipid area tended to decrease with increasing PS bead sizes.

### 3.2. Prolonged exposure of C. elegans to 1.0-μm PS beads in a multigeneration test

Nematodes from the multigeneration test were continuously exposed to 5.49 mg 1.0-μm PS beads $l^{-1}$. After 21 days, lipid droplet distribution differed significantly from that in the unexposed control. There was no significant difference in the amount of lipid droplets (T = 93.000, p = 0.384; Fig. 3A), but in PS-bead-exposed *C. elegans* the lipid droplets were significantly larger (+74%; T < 73.000, p < 0.017; Fig. 3B and C) and covered a significantly larger proportion of the nematode body (+70%; T = 74.000, p = 0.021; Fig. 3D).

### 3.3. Cultivation of C. elegans at ideal and restricted food densities

In *C. elegans* cultivated at restricted food densities, both the number (+85%; T = 195.000, p < 0.001; Fig. 4A) and size (+43%; T < 195.000, p < 0.002; Fig. 4B and C) of the lipid droplets were significantly larger and a larger body area was covered by the droplets (+96%; T = 195.000, p < 0.001; Fig. 4D).

## 4. Discussion

Feeding provides organisms with an adequate supply of nutrients to support growth and maintain cellular functions. According to Stuhr and Curran (2020), the bacterial diet of *C. elegans* has numerous effects on important life-history traits, such as development, reproduction, and longevity (Hansen et al., 2014; Soukas et al., 2009). Other effects include behavior, metabolic profiles, and the nutritional cues perceived in the intestine that regulate fat storage levels (Brooks et al., 2009; Soukas et al., 2009; Watson et al., 2013; You et al., 2008) implying that lipid storage is directly linked with feeding efficiency. *Caenorhabditis elegans* stores fat in lipid droplets in its intestinal and hypodermal cells, which perform essential functions for lipid synthesis and utilization (Ashrafi, 2007). The stored lipids serve as a major energy reserve and can be transferred to embryos in the form of yolk to support progeny development (Li et al., 2020).

Our CARS analyses showed that lipid storage distribution was significantly increased in *C. elegans*, when individuals were exposed to effective concentrations of PS beads, both in chronic toxicity tests (Mueller et al., 2020b) and in the long-term multigeneration test (Mueller et al., 2020a). Although effective concentrations for each respective bead size were similar (EC50), lipid storage analyses further revealed a trend to higher lipid contents in *C. elegans* exposed to PS beads of decreasing size, except of 0.1-μm PS beads inducing significantly different lipid droplet distributions. As a basis for discussion, our results must be put in context to the results of Mueller et al. (2020b). They reported increased toxicities, evidenced as an inhibition of reproduction, in nematodes exposed to PS beads, with smaller beads having greater inhibitory effects on reproduction. The ability of artificial beads to interfere with the feeding of *C. elegans* on its bacterial diet was later confirmed by Rauchschwalbe et al. (2021). The authors found that bacterial consumption was significantly reduced in the presence of PS beads (by up to 67% compared to the control). The effect mechanism differed depending on the size of the beads. For PS beads in the

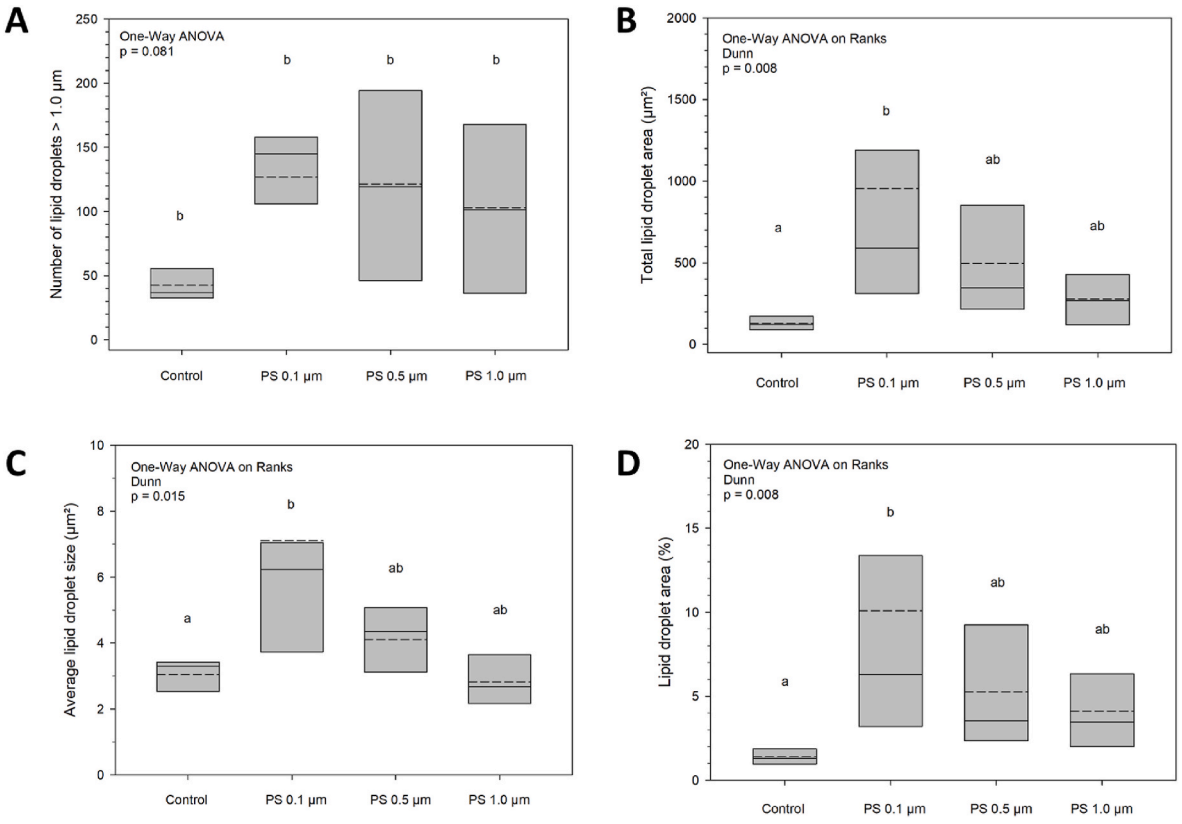


**Fig. 2.** Quantification of lipid storage in an adult *C. elegans* after a 96-h chronic toxicity test (in which the nematode grew from J1 to adult). The nematodes were exposed to PS beads of 0.1, 0.5 and 1.0 μm in diameter at exposure concentrations of 54.9 mg $l^{-1}$, 687 mg $l^{-1}$ and 549 mg $l^{-1}$, respectively, that correspond with the effective concentration EC50 of each PS bead size. Z-stacks were analyzed for the lipid droplet count, total lipid droplet area, average lipid droplet size, and the area (%) of the worm's body occupied by lipid droplets. Different letters indicate significant differences. N = 7. SigmaPlot 12.0 (Systat Software Inc.).

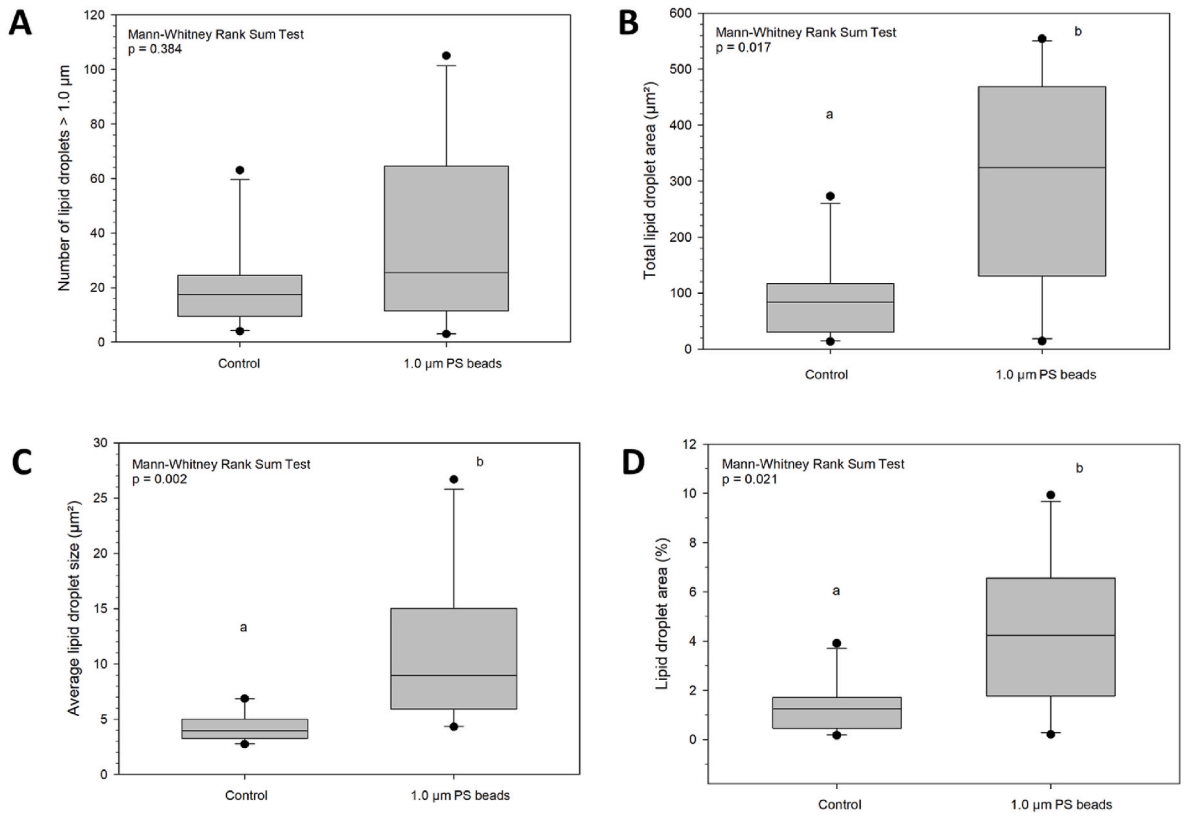


**Fig. 3.** Quantification of lipid storage in an adult *C. elegans* derived from the multigeneration test. The nematodes were exposed to 5.49 mg 1.0-µm PS beads $l^{-1}$ for 21 days. Z-stacks were analyzed for the lipid droplet count, total lipid droplet area, average lipid droplet size, and the percentual area of the worm that was covered with lipid droplets. Different letters indicate significant differences. N = 10. SigmaPlot 12.0 (Systat Software Inc.).

ingestible size range (≤3 µm), the findings were attributed to the dilution of food by the beads and the resulting dietary restriction, as the presence of the beads in the medium prevented the nematodes from consuming the same number of bacterial cells in a given time as in the absence of beads (Rauchschwalbe et al., 2021). Since PS beads have no nutritional value, the result was a temporal dietary restriction leading to increased lipid storage, reflecting the energy trade-off between reproductive output and upregulated lipid accumulation to cope with the stress.

In accordance to literature, increased fat accumulation is observed in *C. elegans* subjected to high levels of (environmental) stress, consistent with the regulation of stress-resistance mechanisms by fatty-acid metabolism (Horikawa and Sakamoto, 2009). In nematodes, food deficiencies led to imbalanced fat degradation and synthesis that extended the lifespan, increased stress resistance, and reduced individual body size and influenced fat levels (Bar et al., 2016; Li et al., 2020). Generally, in response to unfavorable environmental conditions and stress, including dietary restriction, *C. elegans* larvae can undergo dauer arrest at the second molt (Hu, 2007). Dauer larvae are long-lived and stress-resistant, with an altered metabolism that favors energy conservation, fat storage, and the utilization of stored reservoirs (Ashrafi, 2007). Severe stress can also be induced in *C. elegans* by the exposure to minute particulates since in scanning electron micrographs of the nematode intestine, a larger number of lipid droplets was seen in nematodes exposed to relatively high concentrations of nanogold (14 nm; Bosch et al., 2018), perhaps reflecting disruption of the pathway that breaks down lipids for energy. Zhang et al. (2010) showed that lipid droplet size is dynamic and closely linked to the storage and mobilization of fat, with larger and more numerous lipid droplets possibly caused by genetic defects in a peroxisomal β-oxidation pathway. Wang et al. (2016) similarly showed that iron overload synergistically upregulates lipid uptake and accumulation in *C. elegans*. And, for example, cadmium telluride quantum dots (CdTe QDs) at concentrations of 5–20 mg $L^{-1}$ induced an increase in lipid storage in the intestine of *C. elegans* that was partially due to effects on the molecular basis of fatty acid metabolism and a prolonged defecation cycle length, but not to altered feeding or the release of cadmium ions from the dots (Wu et al., 2016).

The effects of nano- and microplastics on lipid storage and fatty acid metabolism in nematodes have been largely understudied. Yang et al. (2020) investigated the effect of 100-nm PS beads on lipid accumulation and the stress response in *C. elegans*. They found that the beads influenced the expression of lipid-metabolism-related genes and that a 3-day exposure led to the accumulation of very large amounts of lipids. Aside from lowering the bacterial consumption, the mechanism described by Yang et al. (2020) might have also been the case for the 0.1-µm PS beads in our study explaining the significantly stronger effect of 0.1-µm PS beads on lipid droplet distribution in *C. elegans*.

By additionally cultivating nematodes (J1 to adults) at ideal and restricted food densities, we simulated a lack of food during growth and determined the resulting lipid distributions. Nematodes subjected to food deprivation showed retarded growth and development, matured more slowly than nematodes cultured at ideal food densities, laid fewer eggs (data not shown), and had a significantly higher intestinal lipid content. Egg-laying is costly and may have influenced lipid stores, since individuals that matured and laid eggs had fewer lipids, as seen using CARS microscopy. Together with the results of Mueller et al. (2020b), these observations suggest that lipid accumulation occurs in response to unfavorable environmental conditions and the subsequent stress (here, dietary restriction). In their study of zooplankton, Cole et al. (2015) showed that energy assimilated from food is required for growth, physiological maintenance, metabolism, reproduction, and the establishment of energetic reserves (including lipid storage). Thus, under restrictive dietary conditions there will be an energy trade-off between the respective processes to maintain individual fitness.

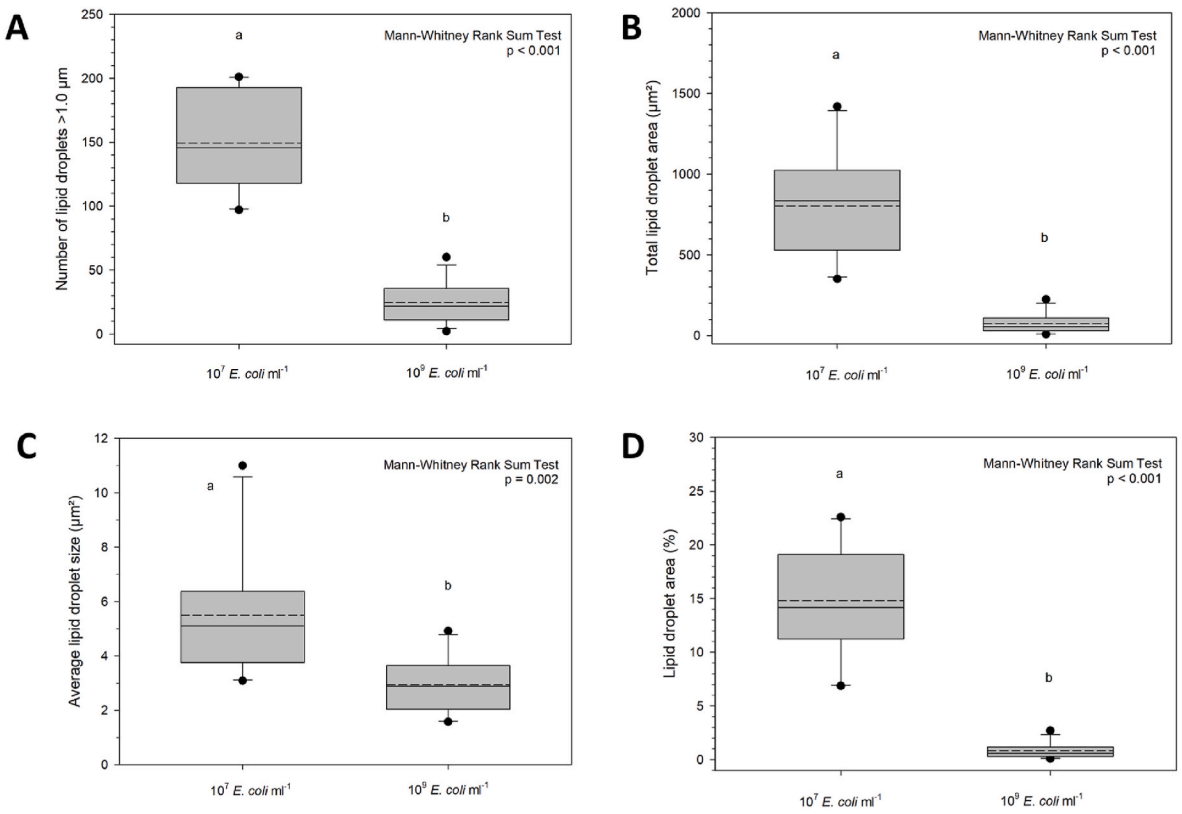


**Fig. 4.** Quantification of lipid storage in adult *Caenorhabditis elegans* cultivated in bacterial (*E. coli*) suspension at either an ideal food density ($10^9$ cells $ml^{-1}$) or under restricted food conditions ($10^7$ cells $ml^{-1}$). Z-stacks were analyzed for the lipid droplet count, the total lipid droplet area, the average lipid droplet size, and the area (%) of the worm's body occupied by lipid droplets. Different letters indicate significant differences. N = 10–14. SigmaPlot 12.0 (Systat Software Inc.).

Effects on energy budgets due to dietary restriction and energy depletion over time in response to MP exposure have been demonstrated in other organisms as well (Cole et al., 2015; Watts et al., 2015; Wright et al., 2013). In the copepod *Calanus helgolandicus*, 20-µm PS beads impeded feeding and led to sustained reductions in ingested carbon biomass (Cole et al., 2015). Budget calculations showed that the MP-exposed copepods had much higher energetic deficiencies and hence reduced growth compared to controls. Polypropylene microfibers (1–5 mm in length, <0.7 mm in diameter) with no nutritional value reduced food consumption by the crab *Carcinus maenas*, with significant reductions in the amount of energy available for growth (Watts et al., 2015). Wright et al. (2013) postulated that the accumulation and prolonged residence times of MPs in the gut underlies the effects of MP-associated dietary restrictions.

## 5. Conclusion

Previous studies showed that the exposure of *C. elegans* to PS beads of a wide range of sizes impedes feeding, by lowering bacterial consumption, which in turn contributes to inhibitory effects on reproduction. In quantitative lipid storage analyses with CARS microscopy, we found that PS beads have an additional influence on the distribution of lipid droplets in *C. elegans* and that the bead size was relevant at similar effective concentrations but played a more subordinate role. While stress-induced lipid storage distribution in *C. elegans* is the same whether the stress is food deprivation or the ingestion of PS beads together with bacterial cells, small PS beads of 0.1 µm showed significantly stronger effects, which might additionally be caused by an altered expression of lipid-metabolism-related genes. The results of this study demonstrate the utility of label-free CARS microscopy in tracking minute MPs ingested by biota and the effects on lipid storage within a single organism, such as other nematode species, chironomids, rotifers, or microalgae (e.g., Jaeger et al., 2016).

## Author statement

**Hendrik Fueser** – Conceptualization, Methodology, Investigation, Data curation, Writing – original draft, Writing – review & editing, Visualization. **Christian Pilger**– Methodology, Investigation, Writing – review & editing, Visualization. **Cihang Kong** – Investigation, Writing – review & editing. **Thomas Huser** – Supervision, Writing – review & editing. **Walter Traunspurger** – Supervision, Writing – review & editing

## Declaration of competing interest

The authors declare that they have no known competing financial interests or personal relationships that could have appeared to influence the work reported in this paper.

## Acknowledgement

We are grateful to Stefanie Gehner for technical assistance and to Dr. Sebastian Höss for insightful remarks on a previous version of this manuscript. This research was supported by the German Federal Ministry of Education and Research (BMBF) as part of the project MikroPlaTaS – Microplastics in Dams and Reservoirs: Sedimentation, Spread, Effects (BMBF grant no. 02WPL1448D). *Caenorhabditis elegans* (strain Bristol N2) was kindly provided by the Caenorhabditis Genetic Center supported by the National Institutes of Health – Office of Research Infrastructure Programs (P40OD010440). Christian Pilger and Cihang Kong were supported by the European Unionś 2020 research and innovation program under the Marie Sklodowska-Curie Grant (agreement no. 766181, project DeLIVER).

## Appendix A. Supplementary data

Supplementary data to this article can be found online at https://doi.org/10.1016/j.envpol.2021.118662.

## References


Aljaibachi, R., Laird, W.B., Stevens, F., Callaghan, A., 2020. Impacts of polystyrene microplastics on *Daphnia magna*: a laboratory and a mesocosm study. Sci. Total Environ. 705, 135800. https://doi.org/10.1016/j.scitotenv.2019.135800.

Araujo, C.F., Nolasco, M.M., Ribeiro, A.M.P., Ribeiro-Claro, P.J.A., 2018. Identification of microplastics using Raman spectroscopy: latest developments and future prospects. Water Res. 142, 426–440. https://doi.org/10.1016/j.watres.2018.05.060.

Ashrafi, K., 2007. Obesity and the regulation of fat metabolism. Worm 1–20. https://doi.org/10.1895/wormbook.1.130.1.

Bar, D.Z., Charar, C., Dorfman, J., Yadid, T., Tafforeau, L., Lafontaine, D.L.J., Gruenbaum, Y., 2016. Cell size and fat content of dietary-restricted *Caenorhabditis elegans* are regulated by ATX-2, an mTOR repressor. P. Natl. Acad. Sci. USA. 113 (32), E4620–E4629. https://doi.org/10.1073/pnas.1512156113.

Besseling, E., Wegner, A., Foekema, E.M., van den Heuvel-Greve, M.J., Koelmans, A.A., 2013. Effects of microplastic on fitness and PCB bioaccumulation by the lugworm *Arenicola marina* (L.). Environ. Sci. Technol. 47 (1), 593–600. https://doi.org/10.1021/es302763x.

Blarer, P., Burkhardt-Holm, P., 2016. Microplastics affect assimilation efficiency in the freshwater amphipod *Gammarus fossarum*. Environ. Sci. Pollut. Res. Int. 23 (23), 23522–23532. https://doi.org/10.1007/s11356-016-7584-2.

Bosch, S., Botha, T.L., Jordaan, A., Maboeta, M., Wepener, V., 2018. Sublethal effects of ionic and nanogold on the nematode *Caenorhabditis elegans*. J. Toxicol. 2018, 6218193. https://doi.org/10.1155/2018/6218193.

Boyd, W.A., Cole, R.D., Anderson, G.L., Williams, P.L., 2003. The effects of metals and food availability on the behavior of *Caenorhabditis elegans*. Environ. Toxicol. Chem. 22 (12), 3049–3055. https://doi.org/10.1897/02-565.

Brooks, K.K., Liang, B., Watts, J.L., 2009. The influence of bacterial diet on fat storage in *C. elegans*. PLoS One 4 (10), e7545. https://doi.org/10.1371/journal.pone.0007545.

Chen, W.-W., Lemieux, G.A., Camp, C.H., Chang, T.-C., Ashrafi, K., Cicerone, M.T., 2020. Spectroscopic coherent Raman imaging of *Caenorhabditis elegans* reveals lipid particle diversity. Nat. Chem. Biol. 16 (10), 1087–1095. https://doi.org/10.1038/s41589-020-0565-2.

Cole, M., Lindeque, P., Fileman, E., Halsband, C., Galloway, T.S., 2015. The impact of polystyrene microplastics on feeding, function and fecundity in the marine copepod *Calanus helgolandicus*. Environ. Sci. Technol. 49 (2), 1130–1137. https://doi.org/10.1021/es504525u.

Cole, M., Lindeque, P., Fileman, E., Halsband, C., Goodhead, R., Moger, J., Galloway, T. S., 2013. Microplastic ingestion by zooplankton. Environ. Sci. Technol. 47 (12), 6646–6655. https://doi.org/10.1021/es400663f.

Evans, C.L., Xie, X.S., 2008. Coherent anti-Stokes Raman scattering microscopy: chemical imaging for biology and medicine. Annu. Rev. Anal. Chem. 1, 883–909. https://doi.org/10.1146/annurev.anchem.1.031207.112754.

Fang-Yen, C., Avery, L., Samuel, A.D.T., 2009. Two size-selective mechanisms specifically trap bacteria-sized food particles in *Caenorhabditis elegans*. P. Natl. Acad. Sci. USA. 106 (47), 20093–20096. https://doi.org/10.1073/pnas.0904036106.

Fueser, H., Majdi, N., Haegerbaeumer, A., Pilger, C., Hachmeister, H., Greife, P., Huser, T., Traunspurger, W., 2018. Analyzing life-history traits and lipid storage using CARS microscopy for assessing effects of copper on the fitness of *Caenorhabditis elegans*. Ecotox. Environ. Safe. 156, 255–262. https://doi.org/10.1016/j.ecoenv.2018.03.037.

Fueser, H., Mueller, M.-T., Traunspurger, W., 2020a. Ingestion of microplastics by meiobenthic communities in small-scale microcosm experiments. Sci. Total Environ. 746, 141276. https://doi.org/10.1016/j.scitotenv.2020.141276.

Fueser, H., Mueller, M.-T., Traunspurger, W., 2020b. Rapid ingestion and egestion of spherical microplastics by bacteria-feeding nematodes. Chemosphere 261, 128162. https://doi.org/10.1016/j.chemosphere.2020.128162.

Fueser, H., Mueller, M.-T., Weiss, L., Höss, S., Traunspurger, W., 2019. Ingestion of microplastics by nematodes depends on feeding strategy and buccal cavity size. Environ. Pollut. 255 (Pt 2), 113227. https://doi.org/10.1016/j.envpol.2019.113227.

Galloway, T.S., Cole, M., Lewis, C., 2017. Interactions of microplastic debris throughout the marine ecosystem. Nat. Ecol. Evol. 1 (5), 116. https://doi.org/10.1038/s41559-017-0116.

Hansen, M., Flatt, T., Aguilaniu, H., 2014. Reproduction, fat metabolism, and life span: what is the connection? Cell Metab 19 (6), 1066. https://doi.org/10.1016/j.cmet.2014.05.017.

Heip, C., Huys, R., Vincx, M., Vanreusel, A., Smol, N., Herman, R., Herman, P.M.J., 1990. Composition, distribution, biomass and production of North Sea meiofauna. Neth. J. Sea Res. 26 (2–4), 333–342. https://doi.org/10.1016/0077-7579(90)90095-X.

Hellerer, T., Axäng, C., Brackmann, C., Hillertz, P., Pilon, M., Enejder, A., 2007. Monitoring of lipid storage in *Caenorhabditis elegans* using coherent anti-Stokes Raman scattering (CARS) microscopy. P. Natl. Acad. Sci. USA. 104 (37), 14658–14663. https://doi.org/10.1073/pnas.0703594104.

Horikawa, M., Sakamoto, K., 2009. Fatty-acid metabolism is involved in stress-resistance mechanisms of *Caenorhabditis elegans*. Biochem. Bioph. Res. Co. 390 (4), 1402–1407. https://doi.org/10.1016/j.bbrc.2009.11.006.

Höss, S., Claus, E., Ohe, P.C.von der, Brinke, M., Güde, H., Heininger, P., Traunspurger, W., 2011. Nematode species at risk—a metric to assess pollution in soft sediments of freshwaters. Environ. Int. 37 (5), 940–949. https://doi.org/10.1016/j.envint.2011.03.013.

Hu, P.J., 2007. Dauer. WormBook 1–19. https://doi.org/10.1895/wormbook.1.144.1.

Jaeger, D., Pilger, C., Hachmeister, H., Oberländer, E., Wördenweber, R., Wichmann, J., Mussgnug, J.H., Huser, T., Kruse, O., 2016. Label-free in vivo analysis of intracellular lipid droplets in the oleaginous microalga *Monoraphidium neglectum* by coherent Raman scattering microscopy. Sci. Rep-UK. 6 (1), 35340. https://doi.org/10.1038/srep35340.

Käppler, A., Fischer, D., Oberbeckmann, S., Schernewski, G., Labrenz, M., Eichhorn, K.-J., Voit, B., 2016. Analysis of environmental microplastics by vibrational microspectroscopy: FTIR, Raman or both? Anal. Bioanal. Chem. 408 (29), 8377–8391. https://doi.org/10.1007/s00216-016-9956-3.

Kiyama, Y., Miyahara, K., Ohshima, Y., 2012. Active uptake of artificial particles in the nematode *Caenorhabditis elegans*. J. Exp. Biol. 215 (Pt 7), 1178–1183. https://doi.org/10.1242/jeb.067199.

Lei, L., Wu, S., Lu, S., Liu, M., Song, Y., Fu, Z., Shi, H., Raley-Susman, K.M., He, D., 2018. Microplastic particles cause intestinal damage and other adverse effects in zebrafish *Danio rerio* and nematode *Caenorhabditis elegans*. Sci. Total Environ. 619–620, 1–8. https://doi.org/10.1016/j.scitotenv.2017.11.103.

Li, Y., Ding, W., Li, C.-Y., Liu, Y., 2020. HLH-11 modulates lipid metabolism in response to nutrient availability. Nat. Commun. 11 (1), 5959. https://doi.org/10.1038/s41467-020-19754-1.

Mueller, M.-T., Fueser, H., Höss, S., Traunspurger, W., 2020a. Species-specific effects of long-term microplastic exposure on the population growth of nematodes, with a focus on microplastic ingestion. Ecol. Indicat. 118, 106698. https://doi.org/10.1016/j.ecolind.2020.106698.

Mueller, M.-T., Fueser, H., Trac, L.N., Mayer, P., Traunspurger, W., Höss, S., 2020b. Surface-related toxicity of polystyrene beads to nematodes and the role of food availability. Environ. Sci. Technol. 54 (3), 1790–1798. https://doi.org/10.1021/acs.est.9b06583.

Ogonowski, M., Schür, C., Jarsén, Å., Gorokhova, E., 2016. The effects of natural and anthropogenic microparticles on individual fitness in *Daphnia magna*. PLoS One 11 (5), e0155063. https://doi.org/10.1371/journal.pone.0155063.

Pologruto, T.A., Sabatini, B.L., Svoboda, K., 2003. ScanImage: flexible software for operating laser scanning microscopes. Biomed. Eng. Online 2, 13. https://doi.org/10.1186/1475-925X-2-13.

Rauchschwalbe, M.-T., Fueser, H., Traunspurger, W., Höss, S., 2021. Bacterial consumption by nematodes is disturbed by the presence of polystyrene beads: the roles of food dilution and pharyngeal pumping. Environ. Pollut. 273, 116471. https://doi.org/10.1016/j.envpol.2021.116471.

Ribeiro-Claro, P., Nolasco, M.M., Araújo, C., 2016. Characterization of microplastics by Raman spectroscopy. Compr. Anal. Chem. 75, 119–151. https://doi.org/10.1016/bs.coac.2016.10.001.

Rios Mendoza, L.M., Balcer, M., 2019. Microplastics in freshwater environments: a review of quantification assessment. Trac. Trends Anal. Chem. 113, 402–408. https://doi.org/10.1016/j.trac.2018.10.020.

Rummel, C.D., Jahnke, A., Gorokhova, E., Kühnel, D., Schmitt-Jansen, M., 2017. Impacts of biofilm formation on the fate and potential effects of microplastic in the aquatic environment. Environ. Sci. Technol. Lett. 4 (7), 258–267. https://doi.org/10.1021/acs.estlett.7b00164.

Scherer, C., Weber, A., Stock, F., Vurusic, S., Egerci, H., Kochleus, C., Arendt, N., Foeldi, C., Dierkes, G., Wagner, M., Brennholt, N., Reifferscheid, G., 2020. Comparative assessment of microplastics in water and sediment of a large European river. Sci. Total Environ. 738, 139866. https://doi.org/10.1016/j.scitotenv.2020.139866.

Schneider, C.A., Rasband, W.S., Eliceiri, K.W., 2012. NIH Image to ImageJ: 25 years of image analysis. Nat. Methods 9 (7), 671–675. https://doi.org/10.1038/nmeth.2089.

Shang, X., Lu, J., Feng, C., Ying, Y., He, Y., Fang, S., Lin, Y., Dahlgren, R., Ju, J., 2020. Microplastic (1 and 5 μm) exposure disturbs lifespan and intestine function in the nematode *Caenorhabditis elegans*. Sci. Total Environ. 705, 135837. https://doi.org/10.1016/j.scitotenv.2019.135837.

Smus, J.P., Ludlow, E., Dallière, N., Luedtke, S., Monfort, T., Lilley, C., Urwin, P., Walker, R.J., O'Connor, V., Holden-Dye, L., Mahajan, S., 2017. Coherent anti-Stokes Raman scattering (CARS) spectroscopy in *Caenorhabditis elegans* and *Globodera pallida*: evidence for an ivermectin-activated decrease in lipid stores. Pest Manag. Sci. 73 (12), 2550–2558. https://doi.org/10.1002/ps.4707.

Soukas, A.A., Kane, E.A., Carr, C.E., Melo, J.A., Ruvkun, G., 2009. Rictor/TORC2 regulates fat metabolism, feeding, growth, and life span in *Caenorhabditis elegans*. Gene Dev. 23 (4), 496–511. https://doi.org/10.1101/gad.1775409.

Stiernagle, T., 2006. Maintenance of *C. elegans*. Worm 1–11. https://doi.org/10.1895/wormbook.1.101.1.

Stuhr, N.L., Curran, S.P., 2020. Bacterial diets differentially alter lifespan and healthspan trajectories in *C. elegans*. Commun. Biol. 3 (1), 653. https://doi.org/10.1038/s42003-020-01379-1.

Traunspurger, W., Höss, S., Witthöft-Mühlmann, A., Wessels, M., Güde, H., 2012. Meiobenthic community patterns of oligotrophic and deep Lake Constance in relation to water depth and nutrients. Fund. Appl. Limnol. 180 (3), 233–248. https://doi.org/10.1127/1863-9135/2012/0144.

Traunspurger, W., Wilden, B., Majdi, N., 2020. An overview of meiofaunal and nematode distribution patterns in lake ecosystems differing in their trophic state. Hydrobiologia 847 (12), 2665–2679. https://doi.org/10.1007/s10750-019-04092-1.

Traunspurger, W. (Ed.), 2021. Ecology of Freshwater Nematodes. CABI Publishing, Wallingford, Boston, MA, ISBN 978-1-78924-363-5, p. 383.

van den Hoogen, J., Geisen, S., Routh, D., Ferris, H., Traunspurger, W., Wardle, D.A., Goede, R.G.M. de, Adams, B.J., Ahmad, W., Andriuzzi, W.S., Bardgett, R.D.,

Bonkowski, M., Campos-Herrera, R., Cares, J.E., Caruso, T., Brito Caixeta, L. de, Chen, X., Costa, S.R., Creamer, R., Mauro da Cunha Castro, J., Dam, M., Djigal, D., Escuer, M., Griffiths, B.S., Gutiérrez, C., Hohberg, K., Kalinkina, D., Kardol, P., Kergunteuil, A., Korthals, G., Krashevska, V., Kudrin, A.A., Li, Q., Liang, W., Magilton, M., Marais, M., Martín, J.A.R., Matveeva, E., Mayad, E.H., Mulder, C., Mullin, P., Neilson, R., Nguyen, T.A.D., Nielsen, U.N., Okada, H., Rius, J.E.P., Pan, K., Peneva, V., Pellissier, L., Carlos Pereira da Silva, J., Pitteloud, C., Powers, T. O., Powers, K., Quist, C.W., Rasmann, S., Moreno, S.S., Scheu, S., Setälä, H., Sushchuk, A., Tiunov, A.V., Trap, J., van der Putten, W., Vestergård, M., Villenave, C., Waeyenberge, L., Wall, D.H., Wilschut, R., Wright, D.G., Yang, J.-I., Crowther, T.W., 2019. Soil nematode abundance and functional group composition at a global scale. Nature 572 (7768), 194–198. https://doi.org/10.1038/s41586-019-1418-6.

Wang, H., Jiang, X., Wu, J., Zhang, L., Huang, J., Zhang, Y., Zou, X., Liang, B., 2016. Iron overload coordinately promotes ferritin expression and fat accumulation in *Caenorhabditis elegans*. Genetics 203 (1), 241–253. https://doi.org/10.1534/genetics.116.186742.

Wang, P., Liu, B., Zhang, D., Belew, M.Y., Tissenbaum, H.A., Cheng, J.-X., 2014. Imaging lipid metabolism in live *Caenorhabditis elegans* using fingerprint vibrations. Angew Chem. Int. Ed. Engl. 53 (44), 11787–11792. https://doi.org/10.1002/anie.201406029.

Watson, E., MacNeil, L.T., Arda, H.E., Zhu, L.J., Walhout, A.J.M., 2013. Integration of metabolic and gene regulatory networks modulates the *C. elegans* dietary response. Cell 153 (6), 1406–1407. https://doi.org/10.1016/j.cell.2013.05.022.

Watts, A.J.R., Lewis, C., Goodhead, R.M., Beckett, S.J., Moger, J., Tyler, C.R., Galloway, T.S., 2014. Uptake and retention of microplastics by the shore crab *Carcinus maenas*. Environ. Sci. Technol. 48 (15), 8823–8830. https://doi.org/10.1021/es501090e.

Watts, A.J.R., Urbina, M.A., Corr, S., Lewis, C., Galloway, T.S., 2015. Ingestion of plastic microfibers by the crab *Carcinus maenas* and its effect on food consumption and energy balance. Environ. Sci. Technol. 49 (24), 14597–14604. https://doi.org/10.1021/acs.est.5b04026.

Welden, N.A.C., Cowie, P.R., 2016. Long-term microplastic retention causes reduced body condition in the langoustine, *Nephrops norvegicus*. Environ. Pollut. 218, 895–900. https://doi.org/10.1016/j.envpol.2016.08.020.

Wendt-Potthoff, K., Imhof, H., Wagner, M., Primpke, S., Fischer, D., Scholz-Böttcher, B., Laforsch, C., 2014. Mikroplastik in binnengewässern. In: Calmano, W., Hupfer, M., Fischer, H., Klapper, H. (Eds.), Handbuch Angewandte Limnologie. Grundlagen - Gewässerbelastung - Restaurierung - Aquatische Ökotoxikologie - Bewertung - Gewässerschutz. Wiley Online Library. Wiley-VCH, Weinheim, pp. 1–35.

Wright, S.L., Rowe, D., Thompson, R.C., Galloway, T.S., 2013. Microplastic ingestion decreases energy reserves in marine worms. Curr. Biol. 23 (23), R1031–R1033. https://doi.org/10.1016/j.cub.2013.10.068.

Wu, Q., Zhi, L., Qu, Y., Wang, D., 2016. Quantum dots increased fat storage in intestine of *Caenorhabditis elegans* by influencing molecular basis for fatty acid metabolism. Nanomedicine-UK 12 (5), 1175–1184. https://doi.org/10.1016/j.nano.2016.01.016.

Yang, Y., Shao, H., Wu, Q., Wang, D., 2020. Lipid metabolic response to polystyrene particles in nematode *Caenorhabditis elegans*. Environ. Pollut. 256, 113439. https://doi.org/10.1016/j.envpol.2019.113439.

Yen, K., Le, T.T., Bansal, A., Narasimhan, S.D., Cheng, J.-X., Tissenbaum, H.A., 2010. A comparative study of fat storage quantitation in nematode *Caenorhabditis elegans* using label and label-free methods. PLoS One 5 (9). https://doi.org/10.1371/journal.pone.0012810.

Yi, Y.-H., Chien, C.-H., Chen, W.-W., Ma, T.-H., Liu, K.-Y., Chang, Y.-S., Chang, T.-C., Lo, S.J., 2014. Lipid droplet pattern and nondroplet-like structure in two fat mutants of *Caenorhabditis elegans* revealed by coherent anti-Stokes Raman scattering microscopy. J. Biomed. Opt. 19 (1), 11011. https://doi.org/10.1117/1.JBO.19.1.011011.

You, Y.-j., Kim, J., Raizen, D.M., Avery, L., 2008. Insulin, cGMP, and TGF-beta signals regulate food intake and quiescence in *C. elegans*: a model for satiety. Cell Metab 7 (3), 249–257. https://doi.org/10.1016/j.cmet.2008.01.005.

Zhang, S.O., Box, A.C., Xu, N., Le Men, J., Yu, J., Guo, F., Trimble, R., Mak, H.Y., 2010. Genetic and dietary regulation of lipid droplet expansion in *Caenorhabditis elegans*. P. Natl. Acad. Sci. USA. 107 (10), 4640–4645. https://doi.org/10.1073/pnas.0912308107.

Zhao, L., Qu, M., Wong, G., Wang, D., 2017. Transgenerational toxicity of nanopolystyrene particles in the range of μg L −1 in the nematode *Caenorhabditis elegans*. Environ. Sci-Nano 4 (12), 2356–2366. https://doi.org/10.1039/C7EN00707H.